Hydrogen bonds *vs.* π-stacking interactions in the *p*-aminophenol···*p*-cresol dimer: an experimental and theoretical study†

M. C. Capello,[a] F. J. Hernández,[a] M. Broquier,[bc] C. Dedonder-Lardeux,[d] C. Jouvet[d] and G. A. Pino*[a]

The gas phase structure and excited state lifetime of the *p*-aminophenol···*p*-cresol heterodimer have been investigated by REMPI and LIF spectroscopy with nanosecond laser pulses and pump–probe experiments with picosecond laser pulses as a model system to study the competition between π–π and H-bonding interactions in aromatic dimers. The excitation is a broad and unstructured band. The excited state of the heterodimer is long lived (2.5 ± 0.5) ns with a very broad fluorescence spectrum red-shifted by 4000 cm^{-1} with respect to the excitation spectrum. Calculations at the MP2/RI-CC2 and DFT-ωB97X-D levels indicate that hydrogen-bonded (HB) and π-stacked isomers are almost isoenergetic in the ground state while in the excited state only the π-stacked isomer exists. This suggests that the HB isomer cannot be excited due to negligible Franck–Condon factors and therefore the excitation spectrum is associated with the π-stacked isomer that reaches vibrationally excited states in the S_1 state upon vertical excitation. The excited state structure is an exciplex responsible for the fluorescence of the complex. Finally, a comparison was performed between the π-stacked structure observed for the *p*-aminophenol···*p*-cresol heterodimer and the HB structure reported for the (*p*-cresol)$_2$ homodimer indicating that the differences are due to different optical properties (oscillator strengths and Franck–Condon factors) of the isomers of both dimers and not to the interactions involved in the ground state.

Introduction

Non-covalent interactions are very important in different areas of chemistry and molecular biology.[1,2] In particular, π–π interactions and hydrogen-bonds (conventional and unconventional H-bonds) between aromatic rings are associated with supramolecular structure and stability of biomolecules, such as proteins[3,4] and nucleic acids,[5,6] as well as important biorecognition processes.[7–9] These non-covalent interactions, in aromatic dimers, can lead to different arrangements such as sandwich (S), parallel displaced (PD), tilted parallel-displaced (T-PD), T-shaped (T), tilted T-shaped (T–T), V-shaped (V) or

[a] *Instituto de Investigaciones en Físico Química de Córdoba (INFIQC) CONICET – UNC. Dpto. de Fisicoquímica – Facultad de Ciencias Químicas – Centro Láser de Ciencias Moleculares – Universidad Nacional de Córdoba, Ciudad Universitaria, X5000HUA Córdoba, Argentina. E-mail: gpino@fcq.unc.edu.ar*

[b] *Centre Laser de l'Université Paris Sud (CLUPS/LUMAT), Univ. Paris-Sud, CNRS, Institut d'Optique Graduate School, Univ. Paris-Saclay, F-91405 Orsay, France*

[c] *Institut des Sciences Moléculaires d'Orsay (ISMO), CNRS, Univ. Paris-Sud, Univ. Paris-Saclay, F-91405 Orsay, France*

[d] *Aix Marseille Université, CNRS, PIIM UMR 7345, Marseille, 13397, France*

† Electronic supplementary information (ESI) available. See DOI: 10.1039/c6cp06352g

hydrogen bond (HB) configurations, depending on the orientation of each ring.[10]

Recent theoretical results on the benzene dimer, a benchmark system to understand π–π interactions, have shown that both S and T structures are almost isoenergetic,[11–14] but only the T configuration has been observed experimentally.[15–17]

The most recent theoretical results on aromatic dimers are focused on analyzing the substituent effects in the π–π interactions, studying complexes of benzene and substituted benzenes.[10,18–22] These studies revealed that all the dimers of substituted benzenes, in the S configuration, bind stronger than the benzene dimer, irrespective of the nature of the substituents, *i.e.*, electron donating or withdrawing.[18,20] This result contradicts the Hunter–Sanders rules proposed to explain the substituent effects on the π–π interactions,[23] and therefore, the electrostatic term is not the sole factor governing the binding energy in these kinds of interactions.

Many studies focus on the competition between different interactions that can occur in complexes of substituted aromatic molecules, especially to characterize the stabilization driving forces of π-stacked and HB dimers.

In some cases, the π-stacked structures have been characterized experimentally and assumed to be the most stable ones in the

ground state of the dimer. Some of these π-stacked dimers involve N-heterocyclic aromatic rings[24–28] while there are a few cases in which π-stacking structures are formed by substituted benzene rings such as the aniline dimer,[29] the 1,2-difluorobenzene dimer,[30] the heterodimers of aniline–benzene[31] and anisole–benzene[32] and more recently the homodimers of phenylacetylene[33] and anisole[34] have also been characterized as π-stacked structures.

In other cases, T, V and HB structures of (phenol)$_2$[35] and (p-cresol)$_2$[36] homodimers, and of 7-azaindole···fluoropyridines,[37] indole···pyridine,[38] indole···imidazole,[39] anisole···phenol,[40] and 7-azaindole···phenol[41] heterodimers have been experimentally observed. These structures are believed to be observed because of their remarkable stability in the ground state, as compared to other possible isomers.

In this work, we present an experimental and theoretical study of the p-aminophenol···p-cresol (p-AmPhOH···p-CreOH) heterodimer that offers the possibility of competition between many kinds of H-bond interactions between different substituents (OH···OH, NH···OH, OH···NH) of both molecules as well as π-stacking interaction between the rings.

Experimental

The experimental set-up used in Córdoba for LIF and REMPI spectroscopy with nanosecond lasers has been described previously.[42] Briefly, the carrier gas He at 1.5 bar passed through two reservoirs, the first one containing p-CreOH at room temperature, and the second one containing p-AmPhOH heated up to 353–385 K. The mixture was co-expanded into a vacuum chamber through a 300 μm diameter pulsed nozzle (Solenoid General Valve, Series 9). Both reactants, p-CreOH and p-AmPhOH, were purchased from Sigma-Aldrich and used without further purification.

LIF and REMPI spectra were recorded using a frequency doubled Sirah dye laser (FWHM = 0.08 cm^{-1}) operating with Rhodamine 590, Rhodamine 610, Rhodamine 640 and DCM, pumped by the second harmonic (532 nm) of a Nd:YAG laser (Quantel, Brilliant B, pulse duration: 6 ns). For the REMPI experiments, the molecular beam was collimated by a skimmer and was crossed perpendicularly by the laser beam in the center of the extraction zone of a home-made Wiley–McLaren time-of-flight (TOF) mass spectrometer (MS) (46 cm flight length). The ions were extracted perpendicularly to the molecular beam and laser directions, and detected using a microchannel plate (Jordan MCP). For the LIF experiments, excitation (LE) and dispersion (DF), the jet was intercepted at the right angle, by the laser beam, at 1.5–2.0 cm from the nozzle. The fluorescence was collected by a telescope collinear to the jet and detected using a photomultiplier tube (PMT) (Hammamatsu R636) without any filter, or dispersed by a monochromator (FWHM = 1 nm). The signals from PMT and MCP were averaged and digitized by a Tektronic (TDS-3034B) oscilloscope and integrated with a PC. The rise time of the complete detection system was 1 ns.

The experimental conditions used in Orsay were the same as in Córdoba. In this case, pump–probe experiments with picosecond laser pulses were performed. The molecular beam was crossed perpendicularly by the laser beams, 10 cm downstream from the nozzle, in the center of the extraction zone of a TOF-MS and the ions were accelerated toward a MCP detector located at the end of a 1.5 m field-free flight tube perpendicular to the jet and laser beam axis.

For the pump–probe experiments, the third harmonic (355 nm) output of a mode-locked picosecond Nd:YAG laser (EKSPLA-SL300) was split into two parts to pump two OPA and SHG systems (EKSPLA-PG411) for obtaining tunable UV light. One of the systems was used as an excitation laser tuned at several frequencies (ν_1) while the other system was tuned to 325 nm and used as an ionization laser (ν_2), keeping its energy at 100 μJ per pulse approximately, while the energy of the ν_1 laser was attenuated to preclude one-color two-photon ionization. The temporal shapes of both pulses were determined in the fitting procedure as Gaussian functions of (15 ± 2) ps FWHM,[43] while the spectral line width was 5 cm^{-1}. The laser pulses were optically delayed between −300 and 800 ps by a motorized stage.

Theoretical calculations

Ab initio calculations were performed using the TURBOMOLE program package,[44] making use of the resolution-of-the-identity (RI) approximation for the evaluation of the electron-repulsion integrals.[45] The equilibrium geometry of the clusters in their ground electronic state (S$_0$) was determined at the MP2 level. The equilibrium geometry of the lowest excited singlet state (S$_1$) and the excitation energies were determined at the RI-CC2 level.[46] These calculations were performed with the correlation-consistent polarized valence double-zeta basis set (cc-pVDZ).[47] The Franck–Condon simulation was performed using the PGOPHER software[48] using the vibrational frequencies calculated for the ground and excited electronic states. Additionally, some faster DFT and TD-DFT calculations were performed using the GAUSSIAN 09 program package,[49] using the ωB97X-D functional[50] and the 6-311G++(d,p) basis set.

Results

Spectroscopy and excited state lifetime of p-AmPhOH···p-CreOH

Fig. 1 shows the one-color REMPI spectra, recorded with nanosecond pulses, of p-AmPhOH, p-CreOH, (p-CreOH)$_2$ and p-AmPhOH···p-CreOH by integrating the intensity of the ions at m/z = 109, 108, 216 and 217 a.m.u., respectively. The spectra of the monomers show narrow and well defined transitions with the band origin (0$_0^0$) for the S$_1$ ← S$_0$ transitions centered at 31 395 cm^{-1} for p-AmPhOH and 35 336 cm^{-1} for p-CreOH. The lowest energy part of the REMPI spectrum of (p-CreOH)$_2$ is also shown in the inset of Fig. 1. The 0$_0^0$ transition for this complex is red-shifted by −324 cm^{-1} from the 0$_0^0$ transition of the free p-CreOH monomer as previously reported.[36] Under the present experimental conditions, well-defined progressions of low-energy vibronic modes are observed for this homodimer. The REMPI spectrum of the p-AmPhOH···p-CreOH complex, recorded with
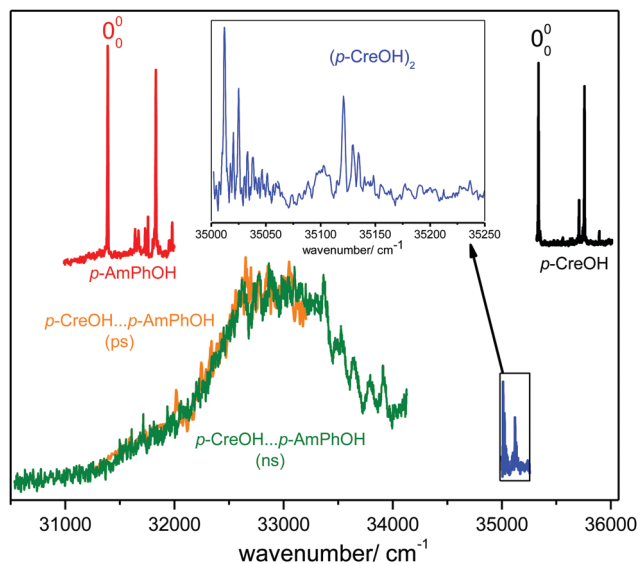
Fig. 1 One-color REMPI spectra of *p*-AmPhOH (red trace), *p*-CreOH (black trace), (*p*-CreOH)$_2$ (blue trace) and *p*-AmPhOH···*p*-CreOH (green trace) recorded with nanosecond pulses. The orange trace corresponds to *p*-AmPhOH···*p*-CreOH REMPI recorded with a picosecond laser. The inset shows an amplification of the (*p*-CreOH)$_2$ spectrum, where well-defined transitions are observed.

Table 1 Lifetimes of *p*-AmPhOH···*p*-CreOH and *p*-AmPhOH measured with picosecond pump–probe experiments and resolved time-laser induced fluorescence (TR-LIF) at different excitation energies. The probe wavelength was 325 nm. The literature lifetime of the lowest energy transition of *p*-CreOH is shown

Complex or molecule	Method	$\lambda_{excitation}/$ nm (cm^{-1})	Lifetime/ns
p-AmPhOH···*p*-CreOH	ps pump–probe	301.7 (33 145.5)	(2.7 ± 0.3)
	ps pump–probe	302.3 (33 079)	(2.0 ± 0.6)
	ps pump–probe	304.7 (32 818)	(2.5 ± 0.3)
	TR-LIF	303.2 (32 981.5)	(2.9 ± 0.1)
	TR-LIF	305.2 (32 765.4)	(2.5 ± 0.1)
p-AmPhOH	—	318.5 (31 395)	(2.20 ± 0.03)[a]
p-CreOH	—	282.99 (35 337)	4.1[b]

[a] Ref. 51. [b] Ref. 52.

structured spectra. This result suggests that the lack of structure in the excitation spectrum of the heterodimer is not due to a short excited state lifetime. In addition, structured spectra has been observed for short excited state lifetime species such as phenol···7-azaindole dimer (30 ± 10 ps)[41] and *o*-aminophenol (35 ± 5 ps).[53] Therefore, the broad unstructured excitation spectrum of the *p*-AmPhOH···*p*-CreOH complex is most likely due to a large geometry change between ground and excited states.

Finally, the dispersed fluorescence (DF) spectrum of the *p*-AmPhOH···*p*-CreOH complex, determined under the same experimental conditions as the REMPI spectrum, is shown in Fig. 2. The DF spectrum (black) is a broad band extending over 8000 cm^{-1} (32 000–24 000) cm^{-1} with the threshold at about 24 000 cm^{-1} and the maximum of the band at about 29 000 cm^{-1}.

Geometry optimization and excitation spectrum simulation

As mentioned above, the broad unstructured excitation spectrum of the *p*-AmPhOH···*p*-CreOH complex may be associated with a
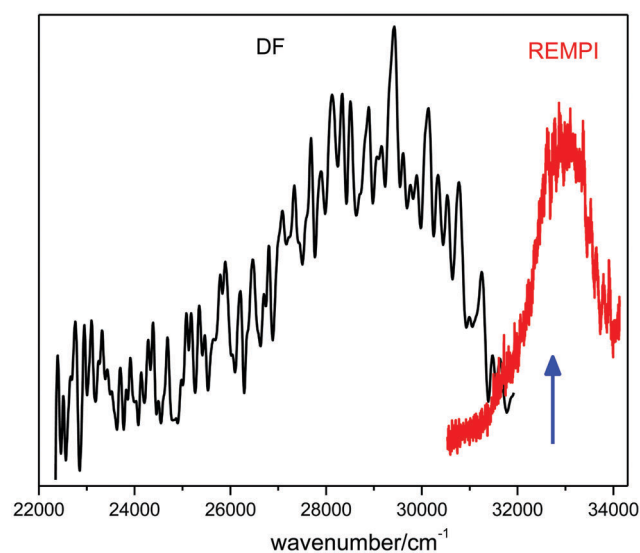
nanosecond pulses (green) and corrected by the dye laser power, is an unstructured broad band extending over 3000 cm^{-1} (31 000 and 34 000 cm^{-1}), with the maximum at approximately 33 000 cm^{-1} and the apparent structure above 33 500 cm^{-1} is due to fluctuations of the laser power. The band origin (0_0^0) for the S$_1$ ← S$_0$ electronic transition cannot be determined in this case. The same broadband spectrum was obtained with picosecond pulses (orange trace).

The broad continuum spectrum may be due to a strong geometry change between the S$_0$ and S$_1$ states or to an ultra-short excited state lifetime of the complex or to hot complexes in the ground state that produce a congested spectrum.

The last possibility can be ruled out since we observed a structured spectrum for (*p*-CreOH)$_2$, which indicates that the clusters formed in the jet are confined in low ro-vibrational levels of the electronic ground state.

To get more information on the excited state lifetime of the *p*-AmPhOH···*p*-CreOH complex, time resolved fluorescence (TR-LIF) experiments with nanosecond lasers as well as pump–probe ionization experiments with picosecond lasers were performed pumping at different excitation wavelengths and probing at 325 nm for the latter case, which is enough to ionize the complex. The different values obtained by both methods are reported in Table 1, together with the excited state lifetimes of the *p*-AmPhOH[51] and *p*-CreOH[52] monomers, reported previously by other authors.

The results show that the average excited state lifetime of the complex, determined by both techniques is (2.5 ± 0.5) ns, without any clear dependence on the excitation energy. Similar excited state lifetimes were reported for the *p*-AmPhOH (2.20 ns)[51] and *p*-CreOH (4.1 ns)[52] monomers, showing well resolved

Fig. 2 Dispersed fluorescence spectrum (DF, black trace) and excitation spectrum (red trace) of (*p*-AmPhOH···*p*-CreOH). The blue arrow indicates the excitation wavelength used to record the DF (32 808.4 cm^{-1}).

31262 | *Phys. Chem. Chem. Phys.*, 2016, **18**, 31260–31267

This journal is © the Owner Societies 2016

marked geometry change between ground and excited state structures of the dimer. Thus, the geometry of the dimer was optimized in both electronic states. The calculations were performed at the DFT-ωB97X-D and MP2 levels of theory for the S_0 state and TD-DFT-ωB97X-D and RI-CC2 levels for the S_1 state. The ωB97X-D functional is currently recommended to evaluate non-covalent complexes and a comparison of the results obtained from the MP2 and DFT methods (see below) supports this recommendation.[54]

A targeted exploration of the potential energy surface was carried out, and multiple trial structures with various bonding motifs, either HB or π-stacked, between both moieties were considered for geometry optimization in the S_0 and S_1 states. The complete set of results is shown in Table S1 (ESI†).

Overall, those structures in which the OH group from *p*-CreOH acts as a H-donor and the NH_2 group of *p*-AmPhOH as a H-acceptor, leading to HB and π-stacked isomers, are the most stable at both theory levels. Hereafter, we will work only on these two isomers since the others are not expected to be present in the molecular beam under the experimental conditions of this work (see Table S1 in the ESI†).

The S_0 state relative energy and the vertical and adiabatic transition energies as well as the optimized structures in the S_0 and S_1 states for the HB and π-stacked isomers, calculated at both theory levels, are shown in Table 2. A good agreement between the results obtained from both theory levels is observed from Table 2, except for the relative stability of the HB and π-stacked isomers in the S_0 state. However, the energy difference is within the

calculation error and therefore it is only an indication that both isomers are almost isoenergetic.
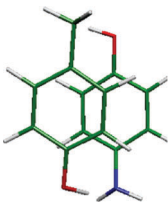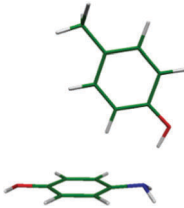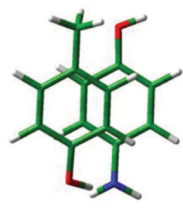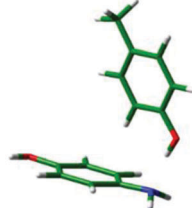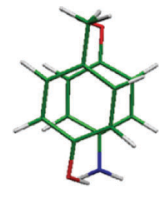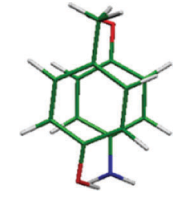
Quite remarkably, geometry optimization in the S_1 state, starting from HB or π-stacked ground state isomers, leads to the same π-stacked (S_1) structure.

For the HB isomer, a large geometry change between the HB (S_0) and π-stacked (S_1) is clearly observed (Table 2) and negligible Franck–Condon factors are expected for its $S_1 \leftarrow S_0$ transition, so it might not be observed by optical excitation. For the π-stacked isomer, the geometry change between π-stacked (S_0) and π-stacked (S_1) is not as large as in the former case. Therefore, although both isomers could be present in the molecular beam, only the π-stacked can be observed.

A close inspection of the S_0 and S_1 state structures of the π-stacked isomer (Fig. 3) shows that while both aromatic rings are displaced in the S_0 state, they are found quite aligned in the S_1 state. In addition, the inter-plane distance is shortened from 3.475 Å in the S_0 state to 2.932 Å in the S_1 state. Finally, the angle between the planes of the rings of both molecules decreases from ~7° to ~4.5°. These geometry changes will induce a large activity of low frequency vibrations in the excitation spectrum and low Franck–Condon factors in the adiabatic excitation region.

The HOMO calculated at the geometry of the S_0 state is a π orbital whose electronic density is distributed almost equally on each ring in such a way that allows the electrostatic interaction between them, while the LUMO calculated at the S_1 geometry is a bonding orbital with most of the electronic density between the rings (Fig. 4).

Table 2 Comparison between the optimized structures of *p*-AmPhOH···*p*-CreOH and energy difference (in eV) between the ground and excited states, calculated at the MP2/RI-CC2/cc-pVDZ and DFT/TD-DFT-ωB97X-D/6-311G++(d,p) levels of theory

	MP2/RI-CC2		DFT/TD-DFT-ωB97X-D	
	π-Stack	HB	π-Stack	HB
Ground state optimized geometry				
Relative energy	0.00	0.06	0.02	0.00
S_0–S_1 vertical transition (without ΔZPE)	4.50	4.60	4.64	4.70
ΔZPE	0.19	—	0.19[a]	0.19[a]
S_0–S_1 vertical transition (with ΔZPE)	4.30	—	4.45	4.51
Excited state optimized geometry				
S_1	3.95	3.88	4.06	4.05
S_0–S_1 adiabatic transition (with ΔZPE)	3.76	3.69	3.87[a]	3.86[a]

[a] ΔZPE was estimated from the MP2/RI-CC2 calculations.

This journal is © the Owner Societies 2016

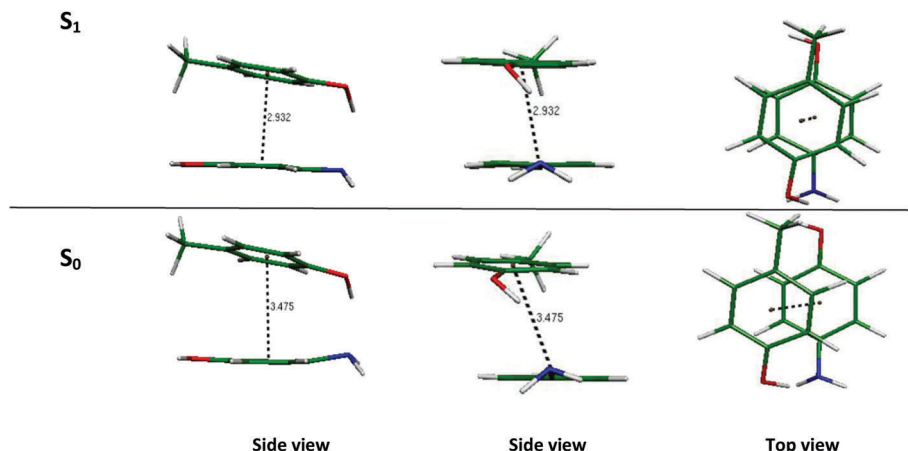*Phys. Chem. Chem. Phys.*, 2016, **18**, 31260–31267 | **31263**

Fig. 3 Optimized structures of *p*-AmPhOH···*p*-CreOH in the ground (S$_0$) and excited state (S$_1$), calculated at the MP2 and RI-CC2 level of theory, respectively. A change in the geometry between these states is clearly observed.

Assuming that the π-stacked isomers are the only one that are optically active in the spectral region explored in this work, the excitation spectrum for the dimer was simulated using the calculated frequencies in the ground and excited states and the Franck–Condon factors computed by the Pgopher program[46] from the optimized geometries of the π-stacked (S$_0$) and π-stacked (S$_1$) at the RI-CC2 level. Fig. 5 shows the simulated (red line) and experimental one-color REMPI ns (black line) spectra of the complex, together with the three most active vibrational modes, which are related to the more important geometry changes between the S$_0$ and S$_1$ states.

A good agreement between the experimental and the simulated spectrum of the π-stacked isomer is presented in Fig. 5. The first band observed in the simulation does not correspond to the 0_0^0 transition but to a higher vibrational level. The 0_0^0 transition is not observed experimentally and according to the simulation

it is expected to be at 3.76 eV (30 328 cm^{-1}), red-shifted by 1067 cm^{-1} from the 0_0^0 transition of bare *p*-AmPhOH.

Discussion

The unstructured spectrum observed for the *p*-AmPhOH···*p*-CreOH complex is not due to spectral congestion associated with bad cooling because the excitation spectrum of the related (*p*-CreOH)$_2$ complex, recorded under the same experimental conditions, is structured. Band broadening associated with a short excited state lifetime was also dismissed as responsible for the lack of structure since for this complex the measured lifetime is (2.5 ± 0.5) ns.

Experimental and theoretical evidence points to a π-stacked isomer that undergoes geometry changes upon electronic excitation. These geometry changes lead to low Franck–Condon factors in the adiabatic excitation energy and then vibrationally excited states are reached in the S$_1$ state producing the unstructured spectrum with negligible intensity in the vicinity of the 0_0^0 transition.

It is clear that the most important changes in geometry between S$_0$ and S$_1$ states are associated with the distance between the aromatic rings and their relative displacement, allowing a better overlap between the π clouds of both molecules in the S$_1$ state than in the S$_0$ state. Moreover, as shown in Fig. 4, the better overlap in the S$_1$ state induces that the electrostatic/dispersive interaction observed between the π clouds in the ground state becomes a bonding orbital with most of the electronic density between the rings in the S$_1$ state, suggesting a stronger interaction between the two aromatic molecules in the excited state, leading to an exciplex-like excited state. These results are in agreement with previous results of other authors on related systems in which a broad excitation spectrum and a red-shifted fluorescence spectrum were associated with the formation of exciplexes.[55–57]
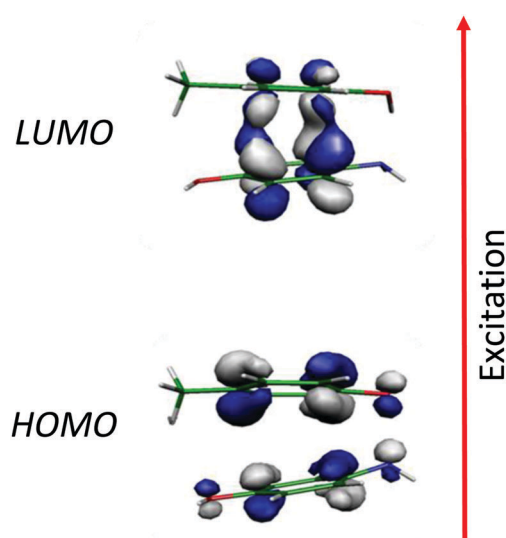
Comparison between *p*-AmPhOH···*p*-CreOH and (*p*-CreOH)$_2$

While this work shows that the π-stacked isomer of the *p*-AmPhOH···*p*-CreOH complex is preferentially observed, the
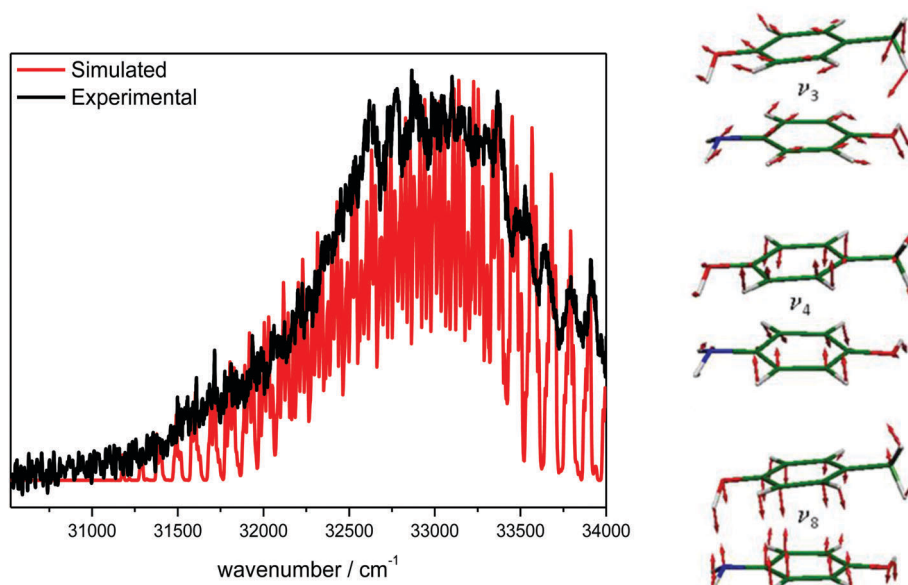

Fig. 4 Orbitals involved in the S$_1$ ← S$_0$ electronic excitation for the *p*-AmPhOH···*p*-CreOH, calculated at the RI-CC2/cc-pVDZ level. In the excited state optimized geometry, an exciplex formation is observed.

Fig. 5 Left panel: Simulated spectra using the ground and excited frequencies calculated at the RI-CC2/cc-pVDZ level for p-AmPhOH$\cdots p$-CreOH. In black, the experimental REMPI spectrum of the dimer recorded with nanosecond pulses. Right panel: Scheme of the most active vibrational modes in the spectrum. The simulated spectrum is less congested than the experimental one since only three vibrational frequencies are included in the simulation due to the exponential increase of the density of state with the number of vibrational modes and the excess energy.

HB isomer was reported to be responsible for the structured excitation spectrum of the homodimer $(p$-CreOH$)_2$,[36] which is in line with the different characteristics of the excitation spectra of these two complexes. These differences may be attributed to different relative stabilization energies of the isomers in each dimer. However, Table 3 shows that π-stacked and HB isomers are isoenergetic at the DFT-ωB97X-D and MP2 levels, in each complex, within the calculation error. Thus, it is expected that the HB as well as the π-stacked isomers of both dimers are present in the molecular beam and at similar concentrations. Therefore, this ground state property should not be the reason for which different isomers are observed in each complex.

Table 3 also shows a good agreement between the experimental transition energies and the calculated adiabatic $S_1 \leftarrow S_0$ transition energies for the assigned isomers. The computed oscillator strength at the TD-DFT (RI-CC2) levels for the HB 0.006 (0.05) and the π-stacked 0.006 (0.02) isomers of the p-AmPhOH$\cdots p$-CreOH complex are very similar and they should be observed with the same probability by means of electronic spectroscopy.

However, the extremely large change in geometry upon excitation of the HB isomers leads to negligible Franck–Condon factors for this transition and then the detection of this isomer becomes unlikely as previously observed in a 7-azaindol$(H_2O)_3$ complex.[43] For the 7-azaindol$(H_2O)_3$ complex, the most stable isomer was not observed due to the large difference between the H-bonded network in the ground and excited state equilibrium geometries that render very weak Franck–Condon factors, and the only isomer observed experimentally is found 0.3 eV above the most stable and unobserved one.

In the case of the $(p$-CreOH$)_2$ complex, the oscillator strength of the transition for the HB isomer 0.06 (0.04) is a factor of 200 (20) larger than the corresponding value for the π-stacked isomer 0.0003 (0.002) at the TD-DFT (RI-ADC2) level, which makes its detection by electronic spectroscopy unlikely. In the π-stacked homodimer, due to the exciton splitting, the first state is optically forbidden as observed from the calculations. The adiabatic transition energy for the first allowed state is found at 5.3 eV at the RI-ADC2 level with an oscillator strength

Table 3 Ground state relative energies, vertical and adiabatic $S_1 \leftarrow S_0$ transition energies (eV) and the corresponding oscillator strengths for the HB and π-stacked isomers of the p-AmPhOH$\cdots p$-CreOH and $(p$-CreOH$)_2$ complexes, calculated at the DFT/TD-DFT-ωB97X-D/6-311G++(d,p) and MP2/RI-CC2/cc-pVDZ (values in parentheses) levels of theory

Isomer	S_0	S_1 vertical	S_1 adiabatic + ΔZPE[a]	Experimental	Osc. strength
p-AmPhOH$\cdots p$-CreOH					
HB	0 (0.06)	4.70 (4.60)	3.86 (3.69)		0.006 (0.05)
π-Stacked	0.02 (0.0)	4.64 (4.50)	3.87 (3.76)	∼3.76	0.006 (0.02)
$(p$-CreOH$)_2$					
HB	0.03 (0.0)	5.01 (4.87)	4.44 (4.46)	4.34	0.06 (0.04)
π-Stacked	0.0 (0.02)	4.97 (4.79)	3.97 (3.92)		0.0003 (0.002)

[a] ΔZPE was estimated (0.19 eV) from the MP2/RI-CC2 calculations.

This journal is © the Owner Societies 2016

Phys. Chem. Chem. Phys., 2016, 18, 31260–31267 | 31265

of 0.05 (RI-ADC2). However, this state is too high in energy to be responsible for the observed experimental transition (4.34 eV). This is assumed to be the reason for which only the HB isomer is observed for this complex.

For a long time many models were developed to explain the effect of the substitution on the preferential HB or π-stacking interaction in aromatic dimers and determine the forces involved.[10,18–22] We show here that the remarkable difference observed upon substituting a CH_3 group by an NH_2 group in one of the p-CreOH molecules of the (p-CreOH)$_2$ dimer can be rationalized considering only the different detection probabilities for HB or π-stacking isomers, without invoking the forces involved in the ground state to stabilize one or the other. In fact, in the ground state both isomers are almost isoenergetic for the homo- and heterodimers.

Finally, it is usually thought that for hydrated clusters, the Franck–Condon factors are not drastically different from those of the chromophore without some photochemistry going on, and as a consequence it is believed that conformation of hydrated clusters is truly restricted to the most stable one (or a few). This assumption has no justification as it is shown in this work and has been already shown previously for the 7-azaindol(H$_2$O)$_3$ complex. Also, in the case of charge transfer states, in which the charge distribution in the excited state is very different, compared to that of the ground state, the equilibrium geometry of a cluster might be quite different between the ground and excited state and thus the Franck–Condon factors can be very low for some isomers and not for others.

It is shown here that a direct relationship between the observation or non-observation of different isomers with their relative stabilities is not always possible, and actually scientifically incorrect unless the Franck–Condon factors, oscillator strengths, excited state lifetimes and ionization efficiencies of all of them are well known.

Conclusions

The gas phase structure of the p-AmPhOH···p-CreOH complex has been studied by REMPI, LIF and pump–probe experiments together with *ab initio* and DFT calculations. From the results it is suggested that a π-stacked structure is responsible for the excitation spectrum. In the excited state this complex behaves as an exciplex-like. Almost isoenergetic with the π-stacked isomer, the HB isomer is not observed due to low Franck–Condon factors.

A comparison with the (p-CreOH)$_2$ dimer for which only the HB isomer was reported indicates that the π-stacked isomer of this complex has an oscillator strength which is too low to be detected by electronic spectroscopy involving this excited state, although in this case, the HB and π-stacked isomers are also almost isoenergetic.

This is another example in which UV and/or IR-UV spectroscopy cannot be employed for searching the most stable structure in the ground state, since the reason for observing or not a given structure depends on the optical properties (oscillator strengths and Franck–Condon factors) of the transition and not only its ground state stability.

References

1 J. Černý and P. Hobza, *Phys. Chem. Chem. Phys.*, 2007, **9**, 5291–5303.
2 P. Auffinger, F. A. Hays, E. Westhof and P. S. Ho, *Proc. Natl. Acad. Sci. U. S. A.*, 2004, **101**, 16789–16794.
3 S. K. Burley and G. A. Petsko, *Science*, 1985, **229**, 23–28.
4 S. Aravinda, N. Shamala, C. Das, A. Sriranjini, I. L. Karle and P. Balaram, *J. Am. Chem. Soc.*, 2003, **125**, 5308–5315.
5 J. Černý, M. Kabeláč and P. Hobza, *J. Am. Chem. Soc.*, 2008, **130**, 16055–16059.
6 P. Yakovchuk, E. Protozanova and M. D. Frank-Kamenetskii, *Nucleic Acids Res.*, 2006, **34**, 564–574.
7 J. Grunenberg, *Phys. Chem. Chem. Phys.*, 2011, **13**, 10136–10146.
8 L. M. Salonen, M. Ellermann and F. Diederich, *Angew. Chem., Int. Ed.*, 2011, **50**, 4808–4842.
9 T. Vacas, F. Corzana, G. Jiménez-Osés, C. González, A. M. Gómez, A. Bastida, J. Revuelta and J. L. Asensio, *J. Am. Chem. Soc.*, 2010, **132**, 12074–12090.
10 C. R. Martinez and B. L. Iverson, *Chem. Sci.*, 2012, **3**, 2191–2201.
11 M. O. Sinnokrot and C. D. Sherrill, *J. Phys. Chem. A*, 2006, **110**, 10656–10668.
12 S. Tsuzuki, K. Honda, T. Uchimaru, M. Mikami and K. Tanabe, *J. Am. Chem. Soc.*, 2002, **124**, 104–112.
13 M. Pitoňák, P. Neogrády, J. Řezáč, P. Jurečka, M. Urban and P. Hobza, *J. Chem. Theory Comput.*, 2008, **4**, 1829–1834.
14 O. Bludský, M. Rubeš, P. Soldán and P. Nachtigallova, *J. Chem. Phys.*, 2008, **128**, 114102.
15 E. Arunan and H. S. Gutowsky, *J. Chem. Phys.*, 1993, **98**, 4294–4296.
16 U. Erlekam, M. Frankowski, G. Meijer and G. von Helden, *J. Chem. Phys.*, 2006, **124**, 171101.
17 M. Miyazaki and M. Fujii, *Phys. Chem. Chem. Phys.*, 2015, **17**, 25989–25997.
18 E. C. Lee, D. Kim, P. Jurečka, P. Tarakeshwar, P. Hobza and K. S. Kim, *J. Phys. Chem. A*, 2007, **111**, 3446–3457.
19 A. L. Ringer and C. D. Sherrill, *J. Am. Chem. Soc.*, 2009, **131**, 4574–4575.
20 M. O. Sinnokrot and C. D. Sherrill, *J. Phys. Chem. A*, 2003, **107**, 8377–8379.
21 J.-I. Seo, I. Kim and Y. S. Lee, *Chem. Phys. Lett.*, 2009, **474**, 101–106.

31266 | *Phys. Chem. Chem. Phys.*, 2016, **18**, 31260–31267

This journal is © the Owner Societies 2016

22 S. A. Arnstein and C. D. Sherrill, *Phys. Chem. Chem. Phys.*, 2008, **10**, 2646–2655.

23 C. A. Hunter and J. K. M. Sanders, *J. Am. Chem. Soc.*, 1990, **112**, 5525–5534.

24 M. Kabeláč, C. Plützer, K. Kleinermanns and P. Hobza, *Phys. Chem. Chem. Phys.*, 2004, **6**, 2781–2785.

25 R. Leist, J. A. Frey, P. Ottiger, H.-M. Frey, S. Leutwyler, R. A. Bachorz and W. Klopper, *Angew. Chem., Int. Ed.*, 2007, **46**, 7449–7452.

26 M. Guin, G. N. Patwari, S. Karthikeyan and K. S. Kim, *Phys. Chem. Chem. Phys.*, 2011, **13**, 5514–5525.

27 M. P. Callahan, Z. Gengeliczki, N. Svadlenak, H. Valdes, P. Hobza and M. S. de Vries, *Phys. Chem. Chem. Phys.*, 2008, **10**, 2819–2826.

28 S. Kumar and A. Das, *J. Chem. Phys.*, 2013, **139**, 104311.

29 N. Yamamoto, K. Hino, K. Mogi, K. Ohashi, Y. Sakai and H. Sekiya, *Chem. Phys. Lett.*, 2001, **342**, 417–424.

30 T. Goly, U. Spoerel and W. Stahl, *Chem. Phys.*, 2002, **283**, 289–296.

31 F. Lahmani, C. Lardeux-Dedonder, D. Solgadi and A. Zehnacker, *Chem. Phys.*, 1988, **120**, 215–223.

32 F. Lahmani, C. Lardeux-Dedonder, D. Solgadi and A. Zehnacker, *J. Phys. Chem.*, 1989, **93**, 3984–3989.

33 S. Maity, G. N. Patwari, R. Sedlak and P. Hobza, *Phys. Chem. Chem. Phys.*, 2011, **13**, 16706–16712.

34 N. Schiccheri, M. Pasquini, G. Piani, G. Pietraperzia, M. Becucci, M. Biczysko, J. Bloino and V. Barone, *Phys. Chem. Chem. Phys.*, 2010, **12**, 13547–13554.

35 R. Brause, M. Santa, M. Schmitt and K. Kleinermanns, *ChemPhysChem*, 2007, **8**, 1394–1401.

36 S. Yan and L. H. Spangler, *J. Phys. Chem.*, 1991, **95**, 3915–3918.

37 S. K. Singh, S. Kumar and A. Das, *Phys. Chem. Chem. Phys.*, 2014, **16**, 8819–8827.

38 S. Kumar, P. Biswas, I. Kaul and A. Das, *J. Phys. Chem. A*, 2011, **115**, 7461–7472.

39 J. G. Hill and A. Das, *Phys. Chem. Chem. Phys.*, 2014, **16**, 11754–11762.

40 G. Pietraperzia, M. Pasquini, F. Mazzoni, G. Piani, M. Becucci, M. Biczysko, D. Michalski, J. Bloino and V. Barone, *J. Phys. Chem. A*, 2011, **115**, 9603–9611.

41 M. C. Capello, M. Broquier, C. Dedonder-Lardeux, C. Jouvet and G. A. Pino, *J. Chem. Phys.*, 2013, **138**, 054304.

42 A. N. Oldani, J. C. Ferrero and G. A. Pino, *Phys. Chem. Chem. Phys.*, 2009, **11**, 10409–10416.

43 G. A. Pino, I. Alata, C. Dedonder, C. Jouvet, K. Sakota and H. Sekiya, *Phys. Chem. Chem. Phys.*, 2011, **13**, 6325–6331.

44 R. Ahlrichs, M. Bär, M. Häser, H. Horn and C. Kölmel, *Chem. Phys. Lett.*, 1989, **162**, 165–169.

45 F. Weigend, M. Häser, H. Patzelt and R. Ahlrichs, *Chem. Phys. Lett.*, 1998, **294**, 143–152.

46 O. Christiansen, H. Koch and P. Jørgensen, *Chem. Phys. Lett.*, 1995, **243**, 409–418.

47 D. E. Woon and T. H. Dunning Jr, *J. Chem. Phys.*, 1993, **98**, 1358–1371.

48 C. M. Western, PGOPHER, a Program for Simulating Rotational Structure, V 7.0.101. Available at http://pgopher.chm.bris.ac.uk, accessed Oct 7, 2013.

49 M. J. Frisch, G. W. Trucks, H. B. Schlegel, G. E. Scuseria, M. A. Robb, J. R. Cheeseman, G. Scalmani, V. Barone, B. Mennucci and G. A. Petersson, *et al.*, *Gaussian 09, Revision D.01*, Gaussian Inc., Wallingford, CT, 2009.

50 J.-D. Chai and M. Head-Gordon, *Phys. Chem. Chem. Phys.*, 2008, **10**, 6615–6620.

51 G. N. Patwari, S. Doraiswamy and S. Wategaonkar, *Chem. Phys. Lett.*, 1999, **305**, 381–388.

52 R. J. Lipert, S. D. Colson and A. Sur, *J. Phys. Chem.*, 1988, **92**, 183–185.

53 M. C. Capello, M. Broquier, S.-I. Ishiuchi, W. Y. Sohn, M. Fujii, C. Dedonder-Lardeux, C. Jouvet and G. A. Pino, *J. Phys. Chem. A*, 2014, **118**, 2056–2062.

54 K. S. Thanthiriwatte, E. G. Hohenstein, L. A. Burns and C. D. Sherrill, *J. Chem. Theory Comput.*, 2011, **7**, 88–96.

55 A. Das, K. K. Mahato and T. Chakraborty, *J. Chem. Phys.*, 2001, **114**, 6107–6111.

56 P. Mitra, B. Chakraborty, D. Bhattacharyya and S. Basu, *J. Phys. Chem. A*, 2013, **117**, 1428–1438.

57 M. Kołaski, C. R. Arunkumar and K. S. Kim, *J. Chem. Theory Comput.*, 2013, **9**, 847–856.

This journal is © the Owner Societies 2016

Phys. Chem. Chem. Phys., 2016, **18**, 31260–31267 | **31267**